

NUMERICAL CALCULATION AND EXPERIMENTAL RESEARCH ON SOUND LOUDNESS IN SOUND FIELD OF STRUCTURAL-ACOUSTIC COUPLING CAVITY

Jixuan Yuan

Original scientific paper

The influence of sound loudness in an enclosed cavity caused by thickness variation of plastic plate, which is simply supported on an enclosed cavity with five rigid walls and excited by a harmonic force, is studied in this article by using numerical algorithms. Based on Finite Element Method (FEM) and Zwicker's Loudness Model, loudness in a structural-acoustic coupled cavity can be obtained by numerical algorithms. An experiment is designed to verify the numerical model. The value of loudness in a cavity with one plastic plate simply supported with its thickness variation is measured by using B&K PULSE 3560C data analysis system. The numerical calculation model is accurate after comparison between numerical calculation result and the experimental result.

Keywords: *experimental research, Finite Element Method (FEM), loudness, structural-acoustic coupling*

Numerički proračun i eksperimentalno istraživanje jačine zvuka u zvučnom polju strukturno-akustički povezane šupljine

Izvorni znanstveni članak

U ovom se radu, primjenom numeričkih algoritama, proučava djelovanje jačine zvuka u zatvorenoj šupljini, promjenom debljine plastične ploče, koju u zatvorenoj šupljini pridržava pet krutih zidova i pobuđuje harmonijska sila. Na temelju metode konačnih elemenata (MKE) i Zwickerova modela glasnoće, glasnoća se u strukturno-akustički povezanoj šupljini može postići numeričkim algoritimima. Postavljen je eksperiment u svrhu provjere numeričkog modela. Vrijednost glasnoće u šupljini s jednom plastičnom pločom promjenljive debljine, izmjerena je primjenom B&K PULSE 3560C sustava za analizu podataka. Točnost numeričkog proračuna modela potvrđena je usporedbom rezultata numeričkog proračuna i rezultata dobivenog eksperimentom.

Ključne riječi: *eksperimentalno istraživanje, glasnoća, metoda konačnih elemenata (MKE), strukturno-akustička povezanost*

1 Introduction

It is very practical and meaningful to study the noise problem inside a cavity. Its application objects include driving cabs of automobile, passenger compartments of a plane and cabins of a ship. With the development of technology, although the noise level in cavity has been improved, many negative reactions caused by "the sound quality in cavity" still exist. Sound quality includes a series of parameters, such as loudness, fluctuation strength and roughness, etc. These parameters influence the human hearing sensation in different ways. The research on sound quality in cavity has theoretical meaning and good use value for low noise and high performance cavity design. This study also has wide application prospect for other engineering problems. Among the parameters of sound quality, loudness is a very important parameter.

Since 1960s, Finite Element Method (FEM) was used to study noise in an enclosed cavity by many researchers. Gladwell and Zimmermann developed an energy formulation of the structural-acoustic theory, in which the stage was set for the application of FEM on acoustic cavity analysis [1]. Early contributions to development of finite element approach were made by Craggs [2], Shuku and Ishihara [3], primarily providing a practical method for analyzing the acoustic of the automobile passenger compartment. And NASTRAN was used by Nefske and Wolf [4] for the study of automobile interior noise, as well as its application into structural-acoustic analyses of the passenger compartment was described.

As for the calculation of sound loudness, on the basis of Zwicker's loudness model [5], researchers provided some methods such as EMBSD [6], PSQM [7], PEAQ [8] and etc. However these methods still failed to provide all

of the necessary details. These were summarized in Ref. [9]. Then Kabla [10] corrected the PEAQ method which was more precise than the others. In the present paper, the corrected PEAQ approach is applied to calculate the sound loudness radiated from rectangular acoustic-structure coupling plates.

Consequently, the sound loudness in an enclosed cavity is thus calculated. By comparing the different thicknesses of the acoustic-structure interaction plates and taking the frequency selectivity of human hearing system into account, the effects of boundary conditions on sound loudness are studied in detail.

2 Zwicker's sound loudness model

The sensation that corresponds most closely to the sound intensity of the stimulus is loudness. Critical bandwidth plays an important role in the loudness, and the loudness on the slopes of the frequency selectivity characteristic of human hearing system may also have essential function. The excitation level versus critical-band rate represents the pattern that describes not only the influence of critical bandwidth but also that of the slopes. Therefore, it seems reasonable to use the excitation level versus critical-band rate as a basis from which the complex of the loudness may be constructed [13]. The loudness is then an integral of the specific loudness over all critical-band rates [5]:

$$N = \int_0^{24} N' dz. \quad (1)$$

Thus, the transformation from critical-band rate level into excitation level versus critical-band rate is necessary.

Both the frequency related transformation into critical-band rate and amplitude related transformation into specific loudness are of crucial importance for evaluating sound at the specific receiver, e.g. the human hearing system. The transformation from excitation level into specific loudness must be known in order to transform excitation level versus critical-band rate into specific loudness versus critical-band rate. This transformation is discussed below.

Steven’s law [13] says that a sensation belonging to the category of intensity sensations grows with physical intensity according to a power law. According to this law, one has to assume that a relative change in loudness is proportional to a relative change in intensity. Instead of the total loudness, specific loudness is used as the value. According to the Zwicker’s loudness model, the specific loudness is given as follow [5]:

$$N' = 0,08 \left(\frac{E_{TQ}}{E_0} \right)^{0,23} \left[\left(0,5 + \frac{0,5E}{E_{TQ}} \right)^{0,23} - 1 \right], \tag{2}$$

Where E_{TQ} is the excitation level at the threshold in quiet approximated by $E_{TQ}(f) = 3,64(f/1000)^{-0,8}$, E_0 is the excitation corresponding to the reference intensity. The values for these two parameters are given in Refs [10].

The critical-band concept is thus important to describe human hearing sensations. And the concept of critical-band rate scale is derived, which is based on the fact that human hearing system analyses a broad spectrum into parts corresponding to critical bands. In many cases, an analytic expression is useful to describe the dependence of the critical-band rate (and of the critical bandwidth) on the frequency over the whole auditory frequency range. The following relations are useful [5]:

$$z = 13 \arctan (0,76 f / 1000) + 3,5 \arctan (f / 7500)^2, \tag{3}$$

and

$$\Delta f_{cr} = 25 + 75 \left[1 + 1,4(f/1000)^2 \right]^{0,69}, \tag{4}$$

where z is critical-band rate, Δf_{cr} is critical bandwidth.

The frequency selectivity of human hearing system can be approximated by subdividing the intensity of the sound into parts that fall into critical band. In order to describe such approximation, the notion of critical-band intensities is put forward. The critical-band level and the excitation level play an important role in many acoustic models. The critical-band level intensity I_{cr} can be calculated from the following equation that takes into account the frequency dependence of critical bandwidth [5]:

$$I_{cr} = \int_{f-0,5\Delta f_{cr}}^{f+0,5\Delta f_{cr}} \frac{dI}{df} df. \tag{5}$$

The critical-band rate z is useful in describing the characteristics of human hearing system. Because the

critical-band rate z is a definite function of frequency, I_{cr} can also be expressed in terms of the critical-band rates as follows:

$$I_{cr} = \int_{z-0,5}^{z+0,5} \frac{dI}{dz} dz. \tag{6}$$

In logarithmic scale, using $I_0 = 10^{-12} \text{ W/m}^2$ as reference value, the critical-band level L_{cr} is defined as follows:

$$L_{cr} = 10 \lg \left(\frac{I_{cr}}{I_0} \right). \tag{7}$$

The critical-band intensity can be seen as that part of the overall un-weighted sound intensity which falls within a frequency window which has the width of a critical band. The transformation of the frequency into the critical-band rate transfers the frequency-dependent window width into a window width of 1 Bark, independent of the critical-band rate. Consequently, a critical-band wide narrow-band noise produces a critical-band intensity which is a function of the critical-band rate, and shows the form of a triangle with a base width of 2-Bark. A harmonic tone, however, produces a function with a rectangular shape and the width of 1 Bark.

The intermediate values such as the excitation or the excitation level, however, represent a much better approximation to the frequency selectivity of human hearing system. The so-called main excitation corresponds in this transformation to the maximum value of the critical-band level. In most cases, the excitation level, defined by L_E , is given by [5]

$$L_E = 10 \lg \left(\frac{E}{E_0} \right). \tag{8}$$

The excitation level can be constructed most simply from the critical-band level as a function of the critical-band rate, by calculating the critical-band level in the range of the main excitation. In cases of an abrupt change of the intensity density as a function of the critical-band rate, as for low-pass noise or sinusoidal tones, the excitation level is identical to the critical-band level.

3 Finite element model for structural-acoustic coupling field

3.1 Discretization of governing equation

FEM (Finite Element Method) based on elements is the most widely-applied numerical method in engineering. According to wave equation of acoustic field:

$$\frac{1}{c^2} \frac{\partial^2 P}{\partial t^2} - \nabla^2 P = 0, \tag{9}$$

where c is sound velocity, $c = \sqrt{k/\rho_0}$, ρ_0 is air density, k is volume modulus of air, P is sound pressure, and t is time.

Because the viscous loss is neglected, Eq. (9) is taken as lossless acoustic wave propagation equation in air. In the problem of acoustic-structure coupling, structural discretization equation and lossless wave equation should be considered together.

For a harmonic mutative sound pressure:

$$P = \bar{P} e^{j\bar{\omega}x}, \tag{10}$$

where \bar{P} is the amplitude of the sound pressure, j is $\sqrt{-1}$, $\bar{\omega}$ is angular frequency, it equals $2\pi f$, and f is the sound pressure vibration frequency.

Putting Eq. (10) into Eq. (9), we get the Helmholtz equation:

$$\frac{\omega^2}{c^2} \bar{P} + \nabla^2 \bar{P} = 0. \tag{11}$$

Eq. (9) is transformed into the following equation:

$$\frac{1}{c^2} \frac{\partial^2 P}{\partial t^2} - \{L\}^T (\{L\}P) = 0, \tag{12}$$

where

$$\{L\}^T = \begin{bmatrix} \frac{\partial}{\partial x} & \frac{\partial}{\partial y} & \frac{\partial}{\partial z} \end{bmatrix}.$$

Through Galerkin method, one can discretize Eq. (12) and get element matrix. And a sound pressure mutative value is multiplied to Eq. (12). By applying volume integral in certain area, one obtains:

$$\int_V \frac{1}{c^2} \delta P \frac{\partial^2 P}{\partial t^2} dV + \int_V (\{L\}^T \delta P) (\{L\}P) dV = \int_S (\{n\}^T \delta P) (\{L\}P) dS, \tag{13}$$

where V is volume, δP is sound pressure mutative value, S is the surface which sound pressure vectors point to, $\{n\}$ is the unit normal vectors of surface S .

In the problem of acoustic-structure coupling interface, normal gradient of sound pressure and structural normal acceleration in fluid momentum equations on interface follow the laws below:

$$\{n\} \cdot \{\Delta P\} = -\rho_0 \{n\} \cdot \frac{\partial^2 \{U\}}{\partial t^2}, \tag{14}$$

where $\{U\}$ is the structural displacement vectors on interface, and matrix representation can be obtained as follows:

$$\{n\}^T \cdot \{\{L\}P\} = -\rho_0 \{n\}^T \left(\frac{\partial^2}{\partial t^2} \{U\} \right). \tag{15}$$

Putting Eq. (15) to Eq. (13):

$$\begin{aligned} & \int_V \frac{1}{c^2} \delta P \frac{\partial^2 P}{\partial t^2} dV + \int_V (\{L\}^T \delta P) (\{L\}P) dV = \\ & = - \int_S \rho_0 \delta P \{n\}^T \left(\frac{\partial^2}{\partial t^2} \{U\} \right) dS. \end{aligned} \tag{16}$$

Approximate shape functions of finite element can be defined as follows:

$$P = \{N\}^T \{P_e\}, \tag{17}$$

$$U = \{N'\}^T \{U_e\}, \tag{18}$$

where $\{N\}$ is the shape function of sound pressure, $\{N'\}$ is the shape function of displacement, $\{P_e\}$ is the sound pressure vector of each node, and $\{U_e\} = \{u_e\}, \{v_e\}, \{w_e\}$ is the displacement vector of each node.

From Eq. (17) and Eq. (18), one can obtain as follows:

$$\frac{\partial^2 P}{\partial t^2} = \{N\}^T \{\ddot{P}\}, \tag{19}$$

$$\frac{\partial^2}{\partial t^2} \{U\} = \{\ddot{U}_e\}, \tag{20}$$

and sound pressure mutative value can be expressed as follows:

$$\delta P = \{N\}^T \{\delta P_e\}. \tag{21}$$

Matrix $[B]$ is defined as follows:

$$[B] = \{L\} \{N\}^T. \tag{22}$$

Putting Eq. (17) and Eq. (22) into Eq. (16), the acoustic wave finite element equation is as follows:

$$\begin{aligned} & \int_V \frac{1}{c^2} \{\delta P_e\}^T \{N\} \{N\}^T dV \{\ddot{P}\} + \int_V (\delta P_e)^T [B]^T [B] dV \{P_e\} + \\ & + \int_S \rho_0 \{\delta P_e\}^T \{N\} \{n\}^T \{N'\} dS \{\ddot{U}\} = \{0\}, \end{aligned} \tag{23}$$

where $\{n\}$ is normal vector of fluid boundary.

Because $\{\delta P\} \neq 0$, $\{\delta P_e\}$ can be divided on both sides of the equation, the non-variables can be moved out from the integral sign:

$$\begin{aligned} & \frac{1}{c^2} \int_V \{N\} \{N\}^T dV \{\ddot{P}\} + \int_V [B]^T [B] dV \{P_e\} + \\ & + \rho_0 \int_S \{N\} \{n\}^T \{N'\} dS \{\ddot{U}\} = \{0\}. \end{aligned} \tag{24}$$

Eq. (24) can also be transformed as follows:

$$[M_e^P] \{\ddot{P}\} + [K_e^P] \{P_e\} + \rho_0 [R_e]^T \{\ddot{U}\} = \{0\}, \tag{25}$$

where $[M_e^P] = \frac{1}{c^2} \int_V \{N\} \{N\}^T dV$, is the mass matrix of the acoustic field fluid; $[K_e^P] = \int_V [B]^T [B] dV$, is the stiffness matrix of the acoustic field fluid; $\rho_0 [R_e]^T = \rho_0 \int_S \{N\} \{n\}^T \{N'\}^T dS$, is the mass matrix of the fluid-structure coupling interface.

Considering the loss energy caused by damping at the fluid boundary, a loss term is added to Eq. (9), and after discretizing with the same method, one obtains:

$$\int_V \frac{1}{c^2} \delta P \frac{\partial^2 P}{\partial t^2} dV - \int_V \delta P \{L\}^T (\{L\} P) dV + \int_S \delta P \left(\frac{r}{\rho_0 c} \right) \frac{1}{c} \frac{\partial P}{\partial t} dS = 0, \tag{26}$$

where r is the sound absorption coefficient of material's damping on the boundary. With the hypothesis that energy is lost only at the boundary of the interface, the energy loss term is integrated at the interface as follows:

$$D = \int_S \delta P \left(\frac{r}{\rho_0 c} \right) \frac{1}{c} \frac{\partial P}{\partial t} dS, \tag{27}$$

where D is the energy loss term, and by putting the shape functions of sound pressure P in Eq. (17) into the energy loss term D , one obtains:

$$D = \int_S \{\delta P_e\}^T \{N\} \left(\frac{r}{\rho_0 c} \right) \frac{1}{c} \{N\}^T dS \left\{ \frac{\partial P_e}{\partial t} \right\}, \tag{28}$$

$\beta = \frac{r}{\rho_0 c}$ is the sound absorption coefficient on the boundary, and $\{\dot{P}_e\}$ represents $\left\{ \frac{\partial P_e}{\partial t} \right\}$.

As the constants on the surface of element, $\frac{\beta}{c}$ and $\{\delta P_e\}$ can be moved out from the integral sign, just as follows:

$$D = \{\delta P_e\}^T \frac{\beta}{c} \int_S \{N\} \{N\}^T dS \{\dot{P}_e\}. \tag{29}$$

Energy loss term is added into Eq. (18), that is to say, the energy loss term on the sound absorption boundary is considered, and

$$[C_e^P] \{\dot{P}_e\} = \frac{\beta}{c} \int_S \{N\} \{N\}^T dS \{\dot{P}_e\}, \tag{30}$$

where $[C_e^P] = \frac{\beta}{c} \int_S \{N\} \{N\}^T dS$ is fluid damping matrix.

Consequently, Eq. (20) is combined with Eq. (25), the discretizing sound wave equation considering the energy loss on the acoustic-structure coupling interface is obtained as follows:

$$[M_e^P] \{\ddot{P}_e\} + [C_e^P] \{\dot{P}_e\} + [K_e^P] \{P_e\} + \rho_0 [R_e]^T \{\dot{U}\} = \{0\}. \tag{31}$$

3.2 Fluid-structure problem in acoustic field

In order to explain the whole fluid-structure problem, fluid sound pressure loads on the interface are added to structural finite element equation shown as follows:

$$[M_e] \{\ddot{U}_e\} + [C_e] \{\dot{U}_e\} + [K_e] \{U_e\} = \{F_e\} + \{F_e^{pr}\}. \tag{32}$$

Sound pressure loads $\{F_e^{pr}\}$ on the interface can be obtained by integrating the sound pressure on the interface:

$$\{F_e^{pr}\} = \int_S \{N'\} P \{n\} dS, \tag{33}$$

where $\{N'\}$ is the structural shape function matrix of discretized displacements u, v, w , $\{n\}$ is the fluid boundary vector.

Putting sound pressure shape function Eq. (17) to Eq. (33):

$$\{F_e^{pr}\} = \int_S \{N'\} \{N\}^T \{n\} dS \{P_e\}. \tag{34}$$

Comparing Eq. (34) with Eq. (25):

$$\{F_e^{pr}\} = [R_e] \{P_e\}, \tag{35}$$

where $[R_e]^T = \int_S \{N'\} \{N\}^T \{n\} dS$.

Putting Eqs. (35) to (32), structural dynamic finite element equation can be obtained as follows:

$$[M_e] \{\ddot{U}_e\} + [C_e] \{\dot{U}_e\} + [K_e] \{U_e\} - [R_e] \{P_e\} = \{F_e\}. \tag{36}$$

Combining Eq. (31) with Eq. (36), the FEM equation of the whole acoustic-structure problem can be obtained as follows:

$$\begin{bmatrix} [M_e] & [0] \\ [M^{fs}] & [M_e^P] \end{bmatrix} \begin{Bmatrix} \{\ddot{U}_e\} \\ \{\ddot{P}_e\} \end{Bmatrix} + \begin{bmatrix} [C_e] & [0] \\ [0] & [C_e^P] \end{bmatrix} \begin{Bmatrix} \{\dot{U}_e\} \\ \{\dot{P}_e\} \end{Bmatrix} + \begin{bmatrix} [K_e] & [K^{fs}] \\ [0] & [K_e^P] \end{bmatrix} \begin{Bmatrix} \{U_e\} \\ \{P_e\} \end{Bmatrix} = \begin{Bmatrix} \{F_e\} \\ \{0\} \end{Bmatrix}, \tag{37}$$

where $[M^{fs}] = \rho_0 [R_e]^T$, $[K^{fs}] = -[R_e]$.

As for the stable acoustic-structure coupling field in an enclosed cavity, sound pressure $P(x, y, z)$ can be obtained by solving Eq. (37) and Eq. (17) at any time. According to the definition of sound intensity [13], sound intensity level L_I is shown as follows:

$$L_I = 20 \cdot \lg \frac{P(x, y, z)}{P_0} + 10 \cdot \lg \frac{400}{\rho_0 c}, \tag{38}$$

where P_0 is the reference sound pressure (2×10^{-5} Pa).

4 Numerical simulation

To investigate the effect of coupling plate thickness on loudness in the enclosed cavity, three kinds of plates with different thicknesses are studied in this section. The thicknesses of the plates are 1 mm, 2 mm, 4 mm.

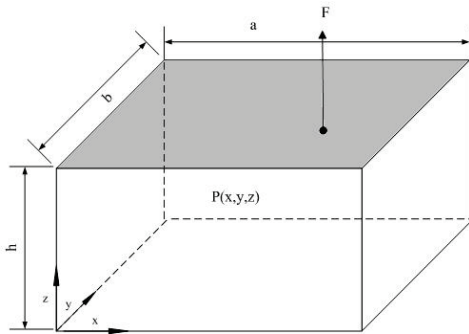


Figure 1 Model of acoustic-structure coupling field

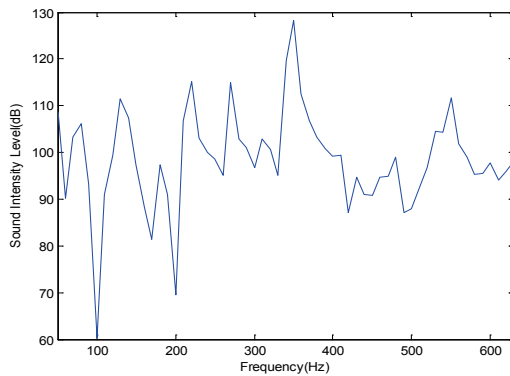


Figure 2(a) Sound intensity level when coupling plate thickness $\delta = 1$ mm

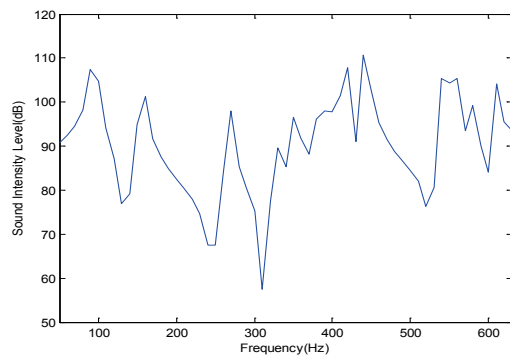


Figure 2(b) Sound intensity level when coupling plate thickness $\delta = 2$ mm

As shown in Fig. 1, one of the cavity boundaries is a rectangular plate with four clamped edges, the colour of the plastic plate shown in Fig. 1 is grey. The other five boundaries are rigid walls. The length of the cavity is $a = 0,5$ m, the width is $b = 0,4$ m, the height is $h = 0,3$ m. The density of the air in the cavity is $\rho_0 = 1,225$ kg/m³, and the sound velocity is $c = 340$ m/s. The material density of the plastic plate is $\rho_s = 2790$ kg/m³, the Poisson ratio is $\nu = 0,3$, the material's loss factor is $\eta = 0$. The exciting force is a harmonic force $f = e^{j\omega t}$, excites the point $(0,4; 0,2; 0,3)$, the observer point is at $(0,1; 0,2; 0,2)$, the frequency range

is between 50 Hz to 630 Hz. The sound intensity level at the observer point is shown in Fig. 2.

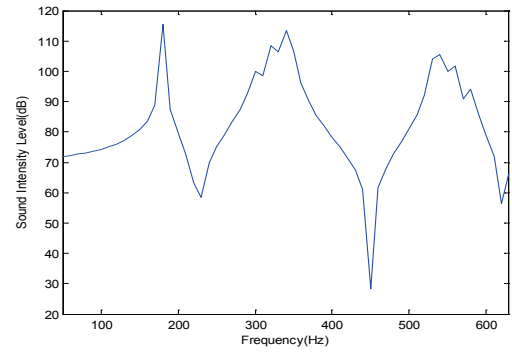


Figure 2(c) Sound intensity level when coupling plate thickness $\delta = 4$ mm

Comparing Figs. 2(a), 2(b) and 2(c), when the thickness of the coupling plate is changed from 1mm to 2 mm, the sound intensity level at the observer point becomes lower. The same trend happens when the thickness is changed from 2 mm to 4 mm. The number of local maximums or local minimums becomes fewer when the thickness is 4 mm. In the low and middle frequency range, when the thickness is 4 mm, frequencies making the sound intensity level maximal or minimal are fewer than those when the thicknesses are 2 mm and 1 mm. The sound intensity level-frequency curve becomes flatter when the frequency increases, and the sound intensity level reaches minimum when the thickness is 4 mm and the frequency is 450 Hz.

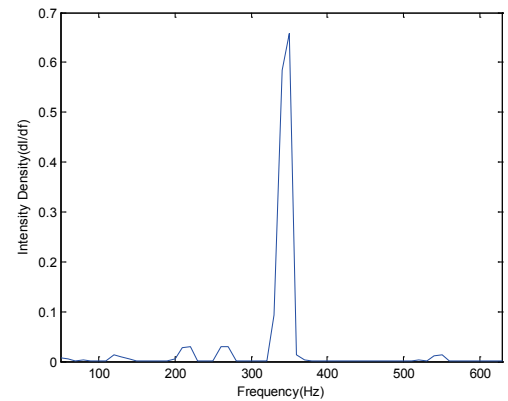


Figure 3(a) Sound intensity density when the coupling plate thickness $\delta = 1$ mm

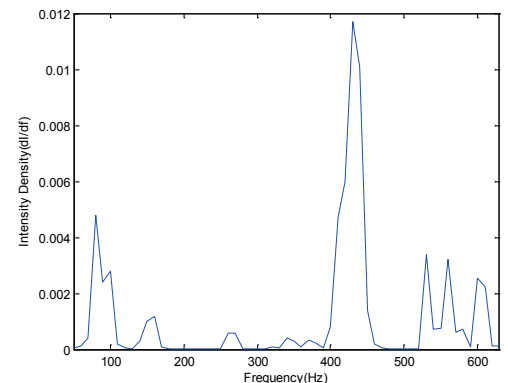


Figure 3(b) Sound intensity density when the coupling plate thickness $\delta = 2$ mm

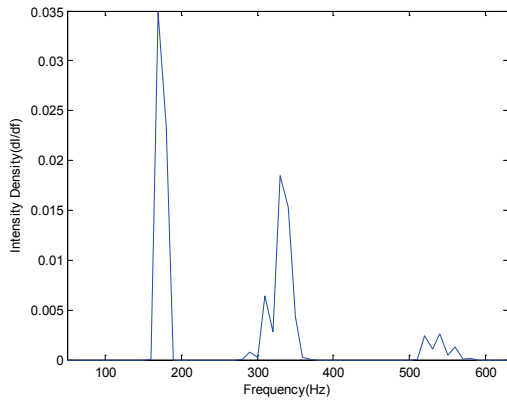


Figure 3(c) Sound intensity density when the coupling plate thickness $\delta = 4$ mm

Because of the frequency selectivity of human hearing system, the sound intensity density dI/df is important in the process of estimating the sound loudness. According to the sound loudness model that has been set up in Section 2, the sound intensity density dI/df can be calculated as shown in Fig. 3.

Each frequency making the sound intensity density maximal or minimal is identical with that making the sound intensity level maximal or minimal in Fig. 2. Except for the proportion of absolute amplitude, the sound intensity density-frequency curve has the same trend as the sound intensity level-frequency curve.

Since the critical-band rate scale is better to describe human hearing sensations and the critical-band rate z is a definite function of frequency, the sound intensity density dI/df can be expressed as by using the critical-band rate scale according to Eq. (3). Once the sound intensity density dI/dz is obtained, then the critical-band level intensity L_{cr} can be calculated according to Eq. (6). Thus, at the observation point, one can obtain the critical-band level L_{cr} caused by different coupling plate thicknesses as shown in Fig. 4.

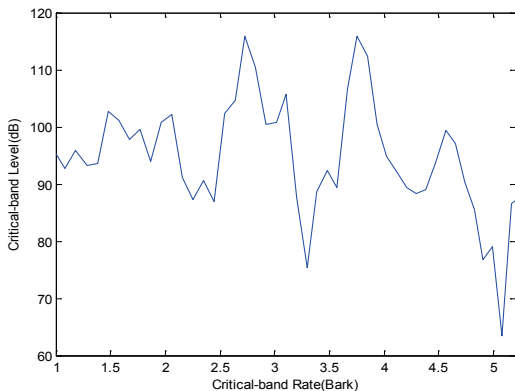


Figure 4(a) Critical-band level when the coupling plate thickness $\delta = 1$ mm

Comparing Fig. 2 and Fig. 4, the critical-band level-bark curves are of great difference in contrast with the sound intensity level-Hz curves in Fig. 2 because human hearing system has frequency selectivity. Note that more frequencies making the critical-band sound intensity level maximal or minimal appear, while the gap between the local maximum and minimum in Fig. 4 is also smaller than that in Fig. 2.

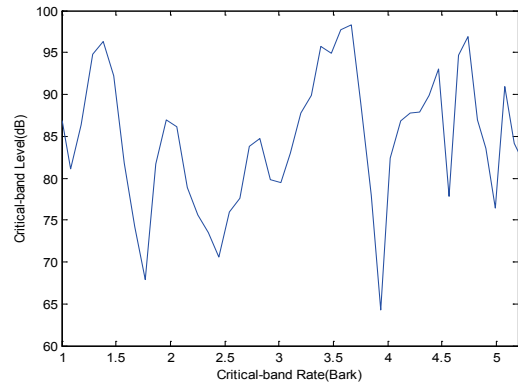


Figure 4(b) Critical-band level when the coupling plate thickness $\delta = 2$ mm

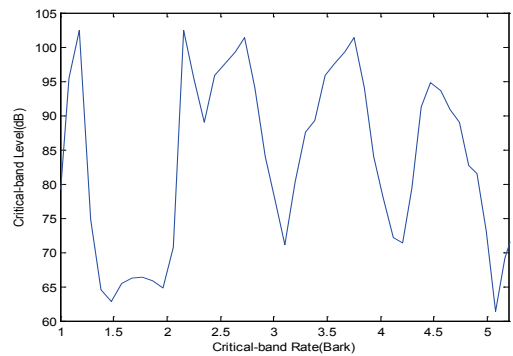


Figure 4(c) Critical-band level when the coupling plate thickness $\delta = 4$ mm

Comparing Figs. 4(a), 4(b) and 4(c), when the coupling plate thickness is changed from 1 mm to 2 mm and from 2 mm to 4 mm, except for the proportion of absolute amplitude, the critical-band level curves are similar when the frequency is above 3 Bark. But there are still differences below 3 Bark, which are very distinct from the ones in Fig. 2.

Eq. (2) is one of the most sophisticated specific loudness calculation methods. The power spectrum of each frame is weighted by the frequency selectivity of the human hearing. The power spectral energies are then grouped into critical bands. An offset is then added to the critical band energies to compensate for internal noise generated in the ear. Because the sound at the observation is harmonic tones, according to Eq. (1) and the transformation of the excitation level from the critical-band level described in Section 2, the sound loudness at the observation point is calculated as shown in Fig. 5.

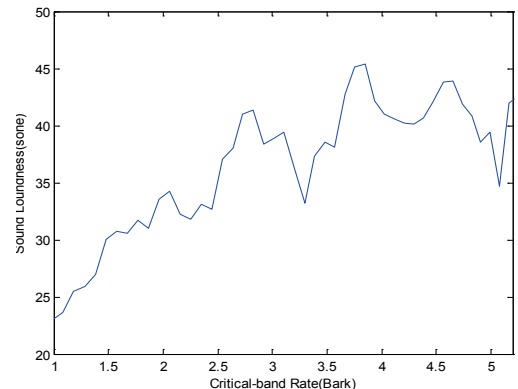


Figure 5(a) Sound loudness when the coupling plate thickness $\delta = 1$ mm

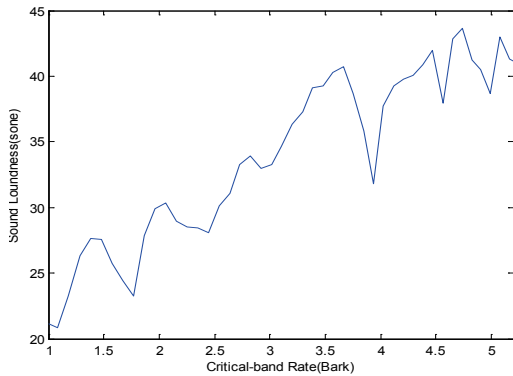


Figure 5(b) Sound loudness when the coupling plate thickness $\delta = 2$ mm

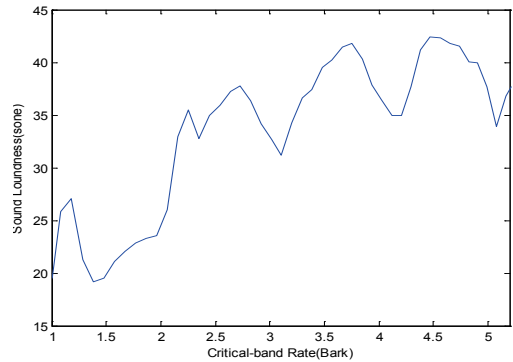


Figure 5(c) Sound loudness when the coupling plate thickness $\delta = 4$ mm

Because of the frequency selectivity of human hearing system, the excitation level at threshold in quiet has different value at different frequency, which is shown in Fig. 6. For this characteristic of human hearing system, the sound loudness obtained at the observation point has low value in low frequency range as shown in Figure 5. On the other hand, though the effect of thickness on the sound loudness is similar to the effect on the critical-band level, there are still great differences.

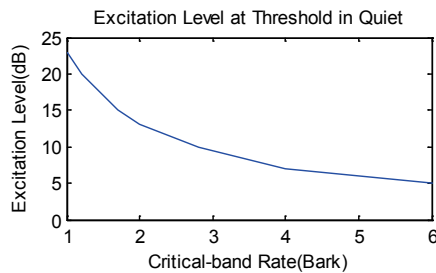


Figure 6 Excitation level at threshold in quiet

Comparing Figs. 5(b) and 5(c), both the value differences and the loudness curve trends are much similar, especially above 3 Bark. At the lower frequency, the loudness value of 2 mm is higher than that of 4 mm, while at the intermediate frequency, the result is opposite. Note that, for the 1 mm plate, some frequencies near 3,5 Bark can make the sound loudness locally minimal, and for 2 mm near 4 Bark, for 4 mm near 3,1 Bark. As for the effect of thickness on the sound loudness obtained at the observation point, it can be seen that the sound loudness of 1 mm is the highest, and the trend of each sound loudness-Bark curve is similar except for the value difference.

5 Experiments

An experiment is designed to prove the sound radiation characteristics in the structural-acoustic coupling system. Five planning wood boards with their 20 mm thickness are regarded as rigid walls of a rectangle cavity and the left wall is composed by a carbon steel plate with thickness of 1mm, and it is simply supported on the rigid walls.

Using PULSE 3560C and data analysis system, a measurement sketch map is as below:

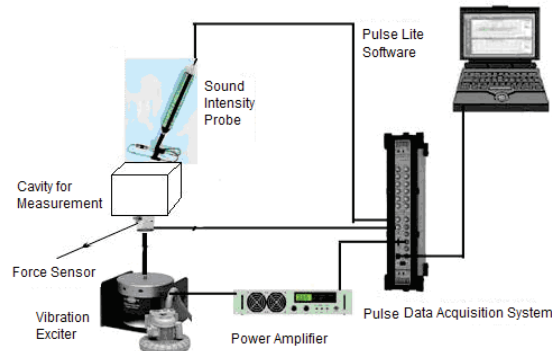


Figure 7 Sound pressure level schematic diagram of experimental system in structural-acoustic coupled system field test



Figure 8 B&K3560 front end, power amplifier, notebook computer and sound intensity probe used in this experiment



Figure 9 Vibration exciter and box structure in this experiment

According to the sound loudness calculation model above, by using the acoustic radiation characteristics, the steel plate's modulus of elasticity is $E = 2,1 \times 10^{11}$ MPa, Poisson's ratio is $\nu = 0,3$, the density of steel is $\rho_s = 7800$ kg/m³, the material damping ratio is $\zeta = 0$. The experiment is carried out in a common room, where air temperature is 25 °C, the relative humidity is 60 %, the air density is $\rho_0 = 1,225$ kg/m³ and the sound velocity is $c = 340$ m/s. At the same time, it is assumed that the cavity is good seal and the sound absorption effect of the wood plank is ignored (regard it as a rigid wall). When the exciting point is at point (0,4; 0,2; 0,3) the point a(0,25;

0,2; 0,15) and point b(0,2; 0,1; 0,15) are chosen as the observation point, the sound intensity level at the observation point a is as follows:

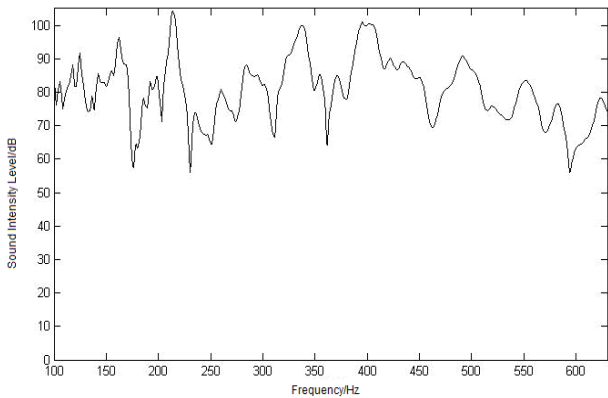


Figure 10 (a) The theoretical value of sound intensity level at point a

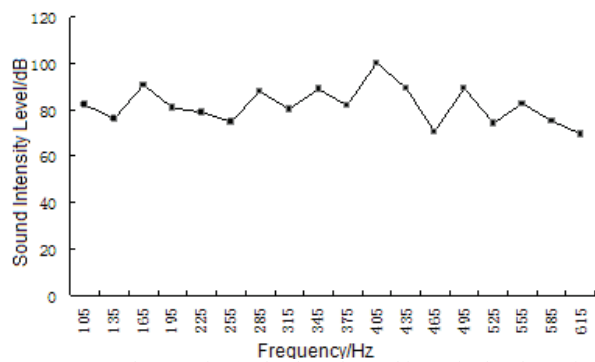


Figure 10 (b) The experimental value of sound intensity level at point a

The sound loudness is transformed from the sound intensity level, the calculating values and the experiment values are as follows:

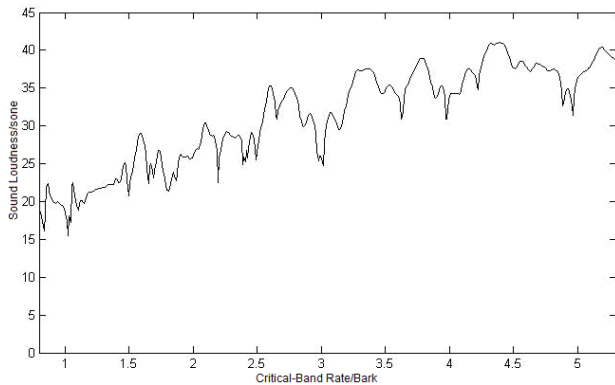


Figure 11 (a) The theoretical value of sound loudness at point a

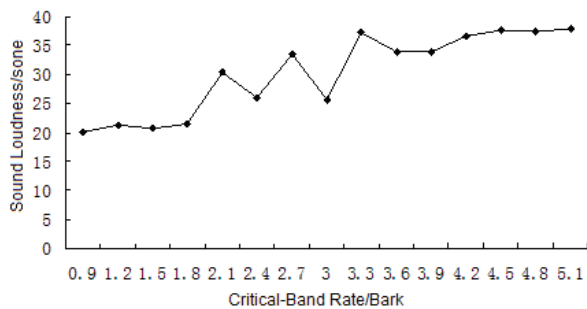


Figure 11 (b) The experimental value of sound loudness at point a

Similarly, the sound intensity values and the sound loudness values at point b are as follows:

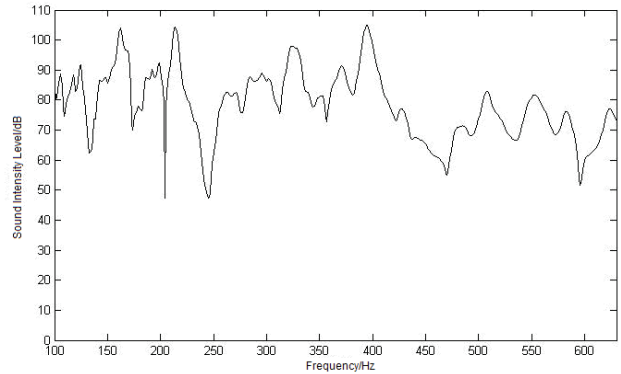


Figure 12 (a) The theoretical value of sound intensity level at point b

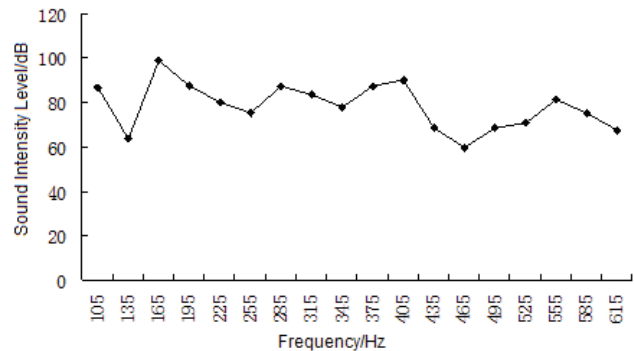


Figure 12 (b) The experimental value of sound intensity level at point b

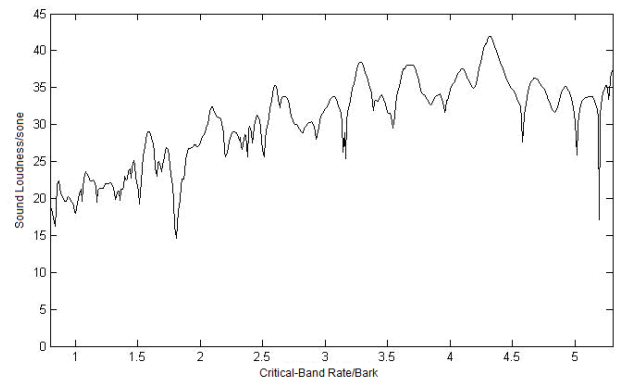


Figure 13 (a) The theoretical value of sound loudness at point b

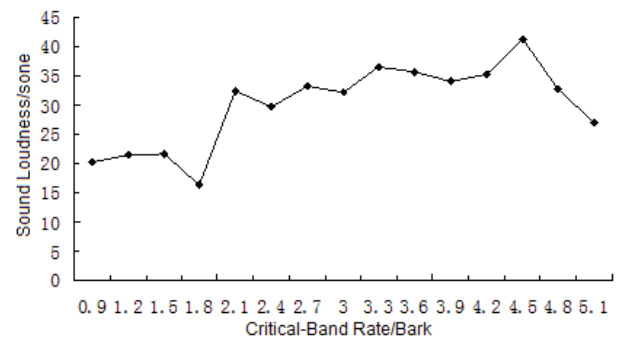


Figure 13 (b) The experimental value of sound loudness at point b

After a contrastive analysis of different sound intensity level values and sound loudness values at different points in the structural-acoustic coupling system, the calculating values basically agree with the experiment values, which shows the calculating method proved in this article is correct.

Furthermore, the difference of sound intensity level between calculation and experiment is less than 3 dB; the difference of sound loudness is less than 0,8 sone, and even most of them are under 0,5 sone. The factors causing the difference are given as below:

1) The vibration exciter will cause sound pressure in the cavity when it is working, and additional mass of the carbon steel plate will be caused by impedance head, therefore some errors happen.

2) The actual dimensions and material properties including density, Young modulus, Poisson's ratio, etc. will be different from the actual parameter, and the difference will cause errors.

3) The boundary conditions of the carbon steel plate are desired to be simply a support, but in fact, it does not match up the ideal boundary conditions.

4) In our experiment, the location of the sound intensity probe may be slightly offset from the location it is desired to be, which gives rise to some errors.

5) The result of experiment is an average value, while the circumstance temperature and humidity are different in each experiment, so some errors would exist.

6 Conclusion

The interior sound field and its sound quality in structural-acoustic coupling system is an important step in modern production and military industry. Many countries and manufacturers are going to do relevant research, such as sound quality in automobile cabin, plane cabin and ship cabin.

An improved sound loudness model in an enclosed cavity is established in this article based on FEM and Zwicker's loudness model. In order to prove the accuracy of the model, some experiments have been conducted and error analysis has been made at last.

According to the results obtained in this article, the sound loudness in the enclosed cavity which is a structural-acoustic coupling field can be calculated in the model and then purposely controlled by applying the coupling plates with different thickness. But when the coupling rectangle plate does not have equal thickness, the sound loudness in the enclosed cavity still needs further study.

Acknowledgments

This work was supported by the Natural Science Foundation of Guangdong Province (Grant No. S2012040007708).

7 References

- [1] Gladwell, C.; Zimmermann, G. On energy and complementary energy formulations of acoustic and structural vibration problem. // *Journal of sound and vibration*. 22, 3(1966), pp. 233-241.
- [2] Craggs, A. The use of simple three-dimensional acoustic finite element for determining the natural modes and frequencies of complex shaped enclosure. // *Journal of sound and vibration*. 23, 4(1972), pp. 331-339.
- [3] Shuku, T.; Ishihara, K. The analysis of the acoustic field in irregular shaped room by the finite element method. // *Journal of sound and vibration*. 29, 7(1973), pp. 67-76.
- [4] Nefske D. J.; Wolf J. A.; Howell L.J. Structural-acoustic finite element analysis of the automobile passenger compartment: a review of current practice. // *Journal of sound and vibration*. 80, 3(1982), pp. 247-266.
- [5] Zwicker, E.; Fastl, H. *Psychoacoustics: Facts and Models*. 2nd Ed. Springer Verlag, Berlin, 1998.
- [6] Wonho, Y. Enhanced Modified Bark Spectral Distortion (EMBSD): An Objective Speech Quality Measure Based on Audible Distortion and Cognition Model. Ph.D. Thesis of Temple University, PA, USA, 1999.
- [7] Colomes, C.; Schmidmer, C.; Thiede, T.; Treurniet, W. C. Perceptual Quality Assessment for Digital Audio: PEAQ-The New ITU Standard for Objective Measurement of the Perceived Audio Quality. // 17th International Conference: High-Quality Audio Coding / Ottawa, Canada, 1999, pp. 33-36.
- [8] Thiede, T. Perceptual Audio Quality Assessment Using a Non-linear Filter Bank. Ph.D. Thesis of TU Berlin, Berlin, Germany, 1999
- [9] Beerends, J. G.; Stemerdink, J. A. A Perceptual Audio Quality Measure Based on a Psychoacoustic Sound Representation. // *Journal of Audio Engineering Society*. 40, 12(1992), pp. 963-978.
- [10] Kabal, P. An Examination and Interpretation of ITU-RBS.1387. Perceptual Evaluation of Audio Quality. TSP Lab Technical Report. 2003, URL: <http://www.mmsp.ece.mcgill.ca/documents/reports/2002/KabalR2002v2.pdf>. (01.06.2014).
- [11] Fastl, H. Evaluation and measurement of perceived average loudness // 5th Oldenburg Symposium on Psychological Acoustics, / Oldenburg, Germany, 1991, pp. 205-216.
- [12] Moore, B. C. *An Introduction to the Psychology of Hearing*. Academic Press, London, 1989.
- [13] Rayleigh, L. *Theory of Sound*. 2nd ed. Dover Publications, New York, 1987.
- [14] Yuan, Jixuan. Application of Sound Loudness Research in Structural Acoustic Coupling Cavity with Impedance and Mobility Approach Method. // *Journal of Vibroengineering*. 15, 4(2013), pp 1898-1912.

Authors' addresses

Jixuan Yuan, Ph.D., Associate Professor
 Shenzhen Institute of Information Technology
 Room 101, Building zhixing No. 3, 2188 Longxiang Boulevard,
 Longgang District, Shenzhen, Guangdong Province, P. R. China
 ZIP code: 518172
 E-mail: yuanjixuan@gmail.com, piyuamn@163.com